

Lanthanide Metal–Organic Frameworks Containing a Novel Flexible Ligand for Luminescence Sensing of Small Organic Molecules and Selective Adsorption

Xiaoqing Wang,^b Liangliang Zhang,^a Jie Yang,^b Fuling Liu,^b Fangna Dai,^a Rongming Wang,^a Daofeng Sun^{*a,b}

^a State Key Laboratory of Heavy Oil Processing, China University of Petroleum (East China), College of Science, China University of Petroleum (East China), Qingdao, Shandong, 266580, People's Republic of China. Email: dfsun@upc.edu.cn.

^b Key Lab of Colloid and Interface Chemistry, Ministry of Education, School of Chemistry and Chemical Engineering, Shandong University, Jinan, Shandong, 250100, People's Republic of China.

Materials and methods

1. Synthesis of ligand H₃L. A mixture of 1,3,5-tris(bromomethyl)-2,4,6-trimethylbenzene (5.2 g, 13 mmol), 4-Methoxycarbonylphenylboronic (9.4 g, 51 mmol), and Pd(PPh₃)₄ (2.2 g, 1.9 mmol) was loaded into a 500 mL Schlenk flask. About 200 mL Na₂CO₃ aqueous solution (2 M) and 150 mL THF were degassed and added through a canula. The solution was heated to 98 °C for 20 hours, and then it was extracted with ethylacetate. The mixture was washed with water and brine, then the organic layer was dried with MgSO₄ and filtered, and the solution was dried on rotary evaporator. The residue was purified with chloroform through a short silica gel column (60% yield). ¹H NMR (300 MHz, CDCl₃): δ/ppm: 2.112 (s, 9H), 3.891(s, 9H), 4.198(s, 6H), 7.101(t, 6H), 7.941(t, 6H).

Then the ester was added in a mixture of THF (20 mL), MeOH (20 mL) and 2 M NaOH aqueous solution (5 mL). The mixture was stirred under reflux for 12 hours, and the solvent was removed under a vacuum. Then dilute HCl was added to the residual aqueous solution until the solution was at pH = 2. The white precipitate was collected by filtration, washed with water, and dried to obtain H₃L (80% yield). ¹H NMR (300 MHz, DMSO): δ/ppm: 2.073 (s, 9H), 4.183(s, 6H), 7.136(t, 6H), 7.869(t, 6H), 12.774(s, 3H).

2. Photoluminescent sensing experiments

2.1 Solvent molecules sensing experiments

The fine grinding sample of **3** (2 mg) was immersed in different organic solvents (3 mL). Then the sample was treated by ultrasonication for 30 min to form a uniform emulsion before the fluorescence study.

2.2 Nitrobenzene derivatives sensing experiments

The fine grinding sample of **3** (2 mg) was immersed in DMSO (3 mL), treated by ultrasonication for 30 min. Then equal volume of aromatic molecules was added into the above samples. Finally, the sample was treated by ultrasonication, which was then added to quartz cuvette. The fluorescence upon excitation at 330 nm was measured in-situ after incremental addition of freshly prepared nitrobenzene derivative solution (1 mmol/L). The emulsion was stirred at constant rate during experiment to maintain homogeneity.

3. The single-site Langmuir-Freundlich model for CO₂ and CH₄ adsorption isotherms

In order to compare the efficiency of complex **5** for CO₂/CH₄ separation, we used the IAST of Myers and Prausnitz along with the pure component isotherm fits to determine the molar loadings in the mixture for specified partial pressures in the bulk gas phase. The measured experimental data on pure component isotherms for CO₂ and CH₄, in terms of excess loadings, were first converted to absolute loading using the Peng-Robinson equation of state for estimation of the fluid densities. The absolute component loadings at 273 K were fitted with a single-site Langmuir-Freundlich model (Equation 1).

$$N = a \times \frac{bp^c}{1+bp^c} \quad (1)$$

Here, *a* is saturation capacity and *b* and *c* are constant. The fitting parameters of equation 1 as well as the correlation coefficients (*R*²) are listed in Table S2.

Table S1. Selected bond length (Å) and angles (°) for complexes **1 -5**.complex **1**

Ce1—O5 ⁱ	2.436 (3)	Ce1—O4 ⁱⁱⁱ	2.418 (3)
Ce1—O6 ⁱⁱ	2.425 (3)	Ce1—O7 ^{iv}	2.491 (3)
Ce1—O1W	2.616 (4)	Ce1—O2	2.488 (3)
Ce1—O3 ^v	2.493 (3)	O5—C24	1.256 (5)
Ce1—O1	2.579 (3)	O6—Ce1 ^{vii}	2.425 (3)
O5—Ce1 ^{vi}	2.436 (3)	O6—C38	1.266 (5)
O5 ⁱ —Ce1—O1W	70.90 (13)	O5 ⁱ —Ce1—O3 ^v	82.13 (11)
O5 ⁱ —Ce1—O7 ^{iv}	139.80 (12)	O5 ⁱ —Ce1—O1	70.30 (13)
O5 ⁱ —Ce1—O2	146.09 (12)	O6 ⁱⁱ —Ce1—O5 ⁱ	85.94 (12)
O6 ⁱⁱ —Ce1—O1W	138.42 (13)	O6 ⁱⁱ —Ce1—O3 ^v	70.32 (11)
O6 ⁱⁱ —Ce1—O7 ^{iv}	117.92 (11)	O6 ⁱⁱ —Ce1—O1	75.72 (12)
O6 ⁱⁱ —Ce1—O2	80.11 (11)	O4 ⁱⁱⁱ —Ce1—O5 ⁱ	92.20 (11)

Symmetry codes: (i) $x+1, y, z+1$; (ii) $x, y, z+1$; (iii) $-x+2, -y, -z+2$; (iv) $-x+3, -y+1, -z+2$; (v) $-x+3, -y+1, -z+3$; (vi) $x-1, y, z-1$; (vii) $x, y, z-1$.

complex **2**

Pr1—O1 ⁱ	2.398 (11)	Pr1—O4 ⁱⁱⁱ	2.463 (11)
Pr1—O5 ⁱⁱ	2.413 (13)	Pr1—O2 ^{iv}	2.459 (11)
Pr1—O6	2.418 (10)	Pr1—O8	2.549 (12)
Pr1—O7	2.593 (13)	O5—Pr1 ⁱⁱ	2.413 (13)
Pr1—O3 ^v	2.464 (11)	O4—Pr1 ^{vii}	2.463 (11)
O1—Pr1 ^{vi}	2.398 (11)	O2—Pr1 ^{iv}	2.459 (11)
O1 ⁱ —Pr1—O5 ⁱⁱ	149.4 (4)	O1 ⁱ —Pr1—O2 ^{iv}	117.4 (4)
O1 ⁱ —Pr1—O6	86.1 (4)	O1 ⁱ —Pr1—O8	76.3 (4)
O1 ⁱ —Pr1—O4 ⁱⁱⁱ	80.5 (4)	O1 ⁱ —Pr1—O7	138.5 (4)
O1 ⁱ —Pr1—O3 ^v	70.0 (4)	O5 ⁱⁱ —Pr1—O2 ^{iv}	82.6 (4)

O5 ⁱⁱ —Pr1—O6	92.0 (4)	O5 ⁱⁱ —Pr1—O8	74.4 (4)
O5 ⁱⁱ —Pr1—O4 ⁱⁱⁱ	84.3 (4)	O5 ⁱⁱ —Pr1—O7	67.9 (5)

Symmetry codes: (i) $x-1, y, z$; (ii) $-x, -y, -z$; (iii) $x-1, y, z-1$; (iv) $-x+1, -y+1, -z$; (v) $-x+1, -y+1, -z+1$; (vi) $x+1, y, z$; (vii) $x+1, y, z+1$.

complex 3

Eu1—O8	2.226 (10)	Eu1—O2 ⁱⁱⁱ	2.337 (7)
Eu1—O8 ⁱ	2.226 (10)	Eu1—O9	2.356 (7)
Eu1—O2 ⁱⁱ	2.337 (7)	Eu1—O1 ^{iv}	2.531 (8)
Eu1—O1 ^v	2.531 (8)	Eu2—O5	2.286 (8)
Eu2—O7 ⁱ	2.268 (10)	Eu2—O6	2.290 (18)
Eu2—O7	2.268 (10)	Eu2—O4 ⁱ	2.349 (10)
O8—Eu1—O8 ⁱ	80.3 (6)	O8—Eu1—O2 ⁱⁱⁱ	76.3 (4)
O8—Eu1—O2 ⁱⁱ	125.2 (5)	O8 ⁱ —Eu1—O2 ⁱⁱⁱ	125.2 (5)
O8 ⁱ —Eu1—O2 ⁱⁱ	76.3 (4)	O2 ⁱⁱ —Eu1—O2 ⁱⁱⁱ	78.2 (3)
O8—Eu1—O9	138.0 (4)	O2 ⁱⁱⁱ —Eu1—O9	88.1 (3)
O8 ⁱ —Eu1—O9	137.6 (4)	O8—Eu1—O1 ^{iv}	117.8 (4)
O2 ⁱⁱ —Eu1—O9	87.9 (3)	O8 ⁱ —Eu1—O1 ^{iv}	73.9 (5)

Symmetry codes: (i) $x, -y+3/2, z$; (ii) $x+1/2, -y+3/2, -z+1/2$; (iii) $x+1/2, y, -z+1/2$; (iv) $x+1/2, -y+3/2, -z+3/2$; (v) $x+1/2, y, -z+3/2$; (vi) $-x+3/2, -y+1, z-1/2$; (vii) $-x+3/2, -y+1, z+1/2$; (viii) $x-1/2, y, -z+1/2$; (ix) $x-1/2, y, -z+3/2$.

complex 4

Tm2—O4	2.257 (10)	Tm2—O2W	2.272 (17)
Tm2—O4 ⁱ	2.257 (10)	Tm2—O5 ⁱ	2.343 (8)
Tm2—O3W	2.261 (17)	Tm2—O5	2.343 (8)
Tm2—O6 ⁱⁱ	2.406 (10)	Tm1—O3 ^{iv}	2.200 (10)
Tm2—O6 ⁱⁱⁱ	2.406 (10)	Tm1—O3 ^v	2.200 (10)
Tm1—O2 ^{vi}	2.39 (3)	Tm1—O2 ^{vii}	2.39 (3)
O4—Tm2—O4 ⁱ	100.0 (6)	O4—Tm2—O2W	79.4 (5)
O4—Tm2—O3W	76.9 (4)	O4 ⁱ —Tm2—O2W	79.4 (5)

O4 ⁱ —Tm2—O3W	76.9 (4)	O3W—Tm2—O2W	142.9 (7)
O4—Tm2—O5 ⁱ	152.2 (4)	O2W—Tm2—O5 ⁱ	127.4 (4)
O4 ⁱ —Tm2—O5 ⁱ	80.6 (4)	O4—Tm2—O5	80.6 (4)
O3W—Tm2—O5 ⁱ	76.1 (4)	O4 ⁱ —Tm2—O5	152.2 (4)

Symmetry codes: (i) $x, -y+3/2, z$; (ii) $-x+3/2, y+1/2, z+1/2$; (iii) $-x+3/2, -y+1, z+1/2$; (iv) $-x+1, y-1/2, -z+1$; (v) $-x+1, -y+1, -z+1$; (vi) $x, -y+1/2, z-1$; (vii) $x, y, z-1$; (viii) $x, -y+1/2, z$; (ix) $-x+3/2, -y+1, z-1/2$; (x) $x, y, z+1$.

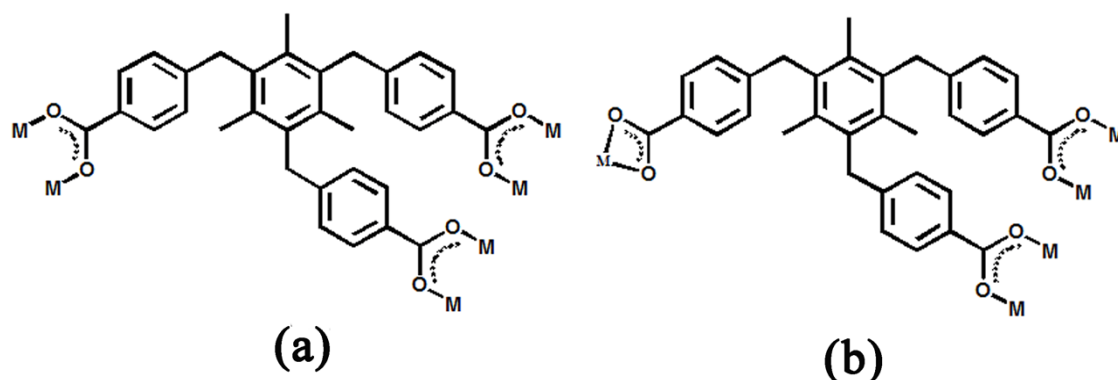
complex 5

Yb1—O6	2.239 (11)	Yb1—O9	2.269 (19)
Yb1—O6 ⁱ	2.239 (11)	Yb1—O8	2.258 (19)
Yb1—O1 ⁱⁱ	2.349 (10)	Yb2—O5	2.204 (11)
Yb1—O1 ⁱⁱⁱ	2.349 (10)	Yb2—O5 ⁱ	2.204 (11)
Yb1—O2 ⁱⁱ	2.379 (11)	Yb2—O3 ^{iv}	2.39 (2)
Yb1—O2 ⁱⁱⁱ	2.379 (11)	Yb2—O3 ^v	2.39 (2)
O6—Yb1—O6 ⁱ	101.3 (7)	O6 ⁱ —Yb1—O2 ⁱⁱⁱ	81.8 (5)
O6 ⁱ —Yb1—O1 ⁱⁱ	153.1 (5)	O6—Yb1—O2 ⁱⁱⁱ	152.6 (5)
O6—Yb1—O1 ⁱⁱ	80.6 (4)	O6—Yb1—O2 ⁱⁱ	81.8 (5)
O6 ⁱ —Yb1—O1 ⁱⁱⁱ	80.6 (4)	O6 ⁱ —Yb1—O9	79.9 (5)
O6—Yb1—O1 ⁱⁱⁱ	153.1 (5)	O6—Yb1—O9	79.9 (5)
O6 ⁱ —Yb1—O2 ⁱⁱ	152.6 (5)	O6—Yb1—O8	77.2 (4)

Symmetry codes: (i) $x, -y+1/2, z$; (ii) $x+1/2, y, -z+1/2$; (iii) $x+1/2, -y+1/2, -z+1/2$; (iv) $x, y, z+1$; (v) $x, -y+1/2, z+1$; (vi) $x-1/2, y, -z+1/2$; (vii) $-x+1, -y+1, -z+1$; (viii) $x, y, z-1$.

Table S2. Equation parameters for the single-site Langmuir-Freundlich model.

Adsorbates	a (mmol/g)	b (kPa ⁻¹)	c	R ²
CO ₂	2.05	0.00884	1.09	0.99999
CH ₄	1.09	0.00145	1.16	0.99998



Scheme S1. Coordinate modes of L^{3-} in complexes 1-5.

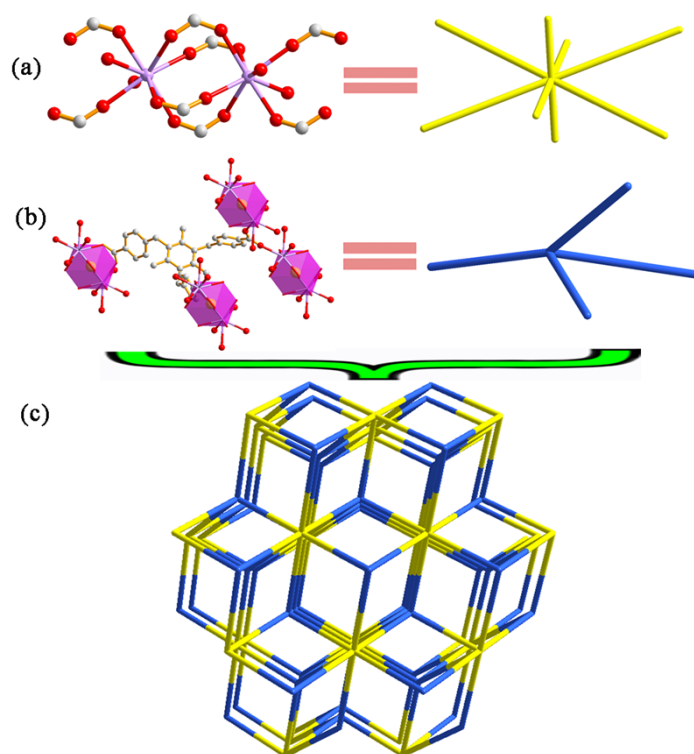


Figure S1. Schematic representations of a simplified 3D network for **1** with *sqc* 169 topology (c) containing 8-connected (a) and 4-connected nodes (b).

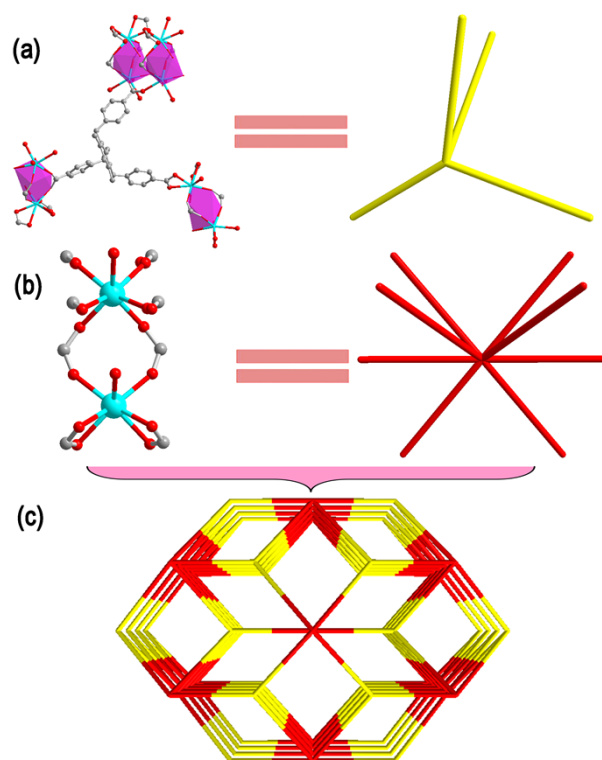


Figure S2. Schematic representations of a simplified 3D network for **4** with 4, 8-connected network (c) containing 4-connected (a) and 8-connected nodes (b).

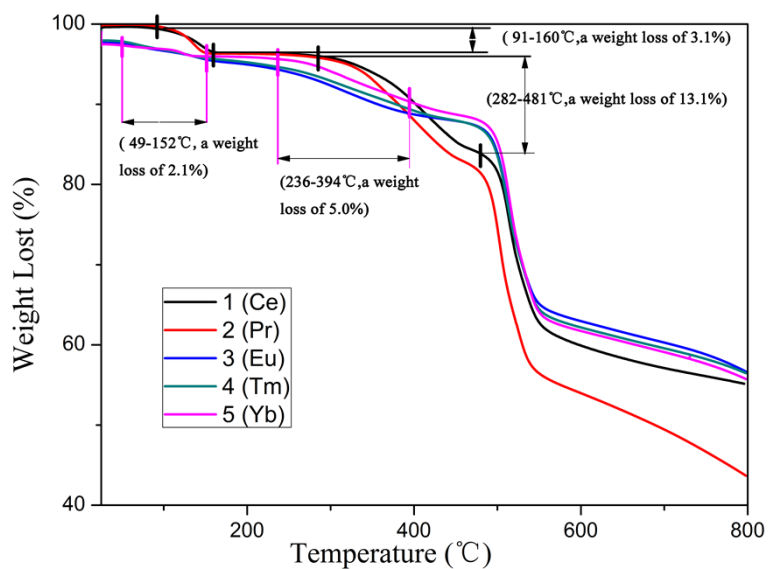


Figure S3. The TGA curves of complexes **1-5**.

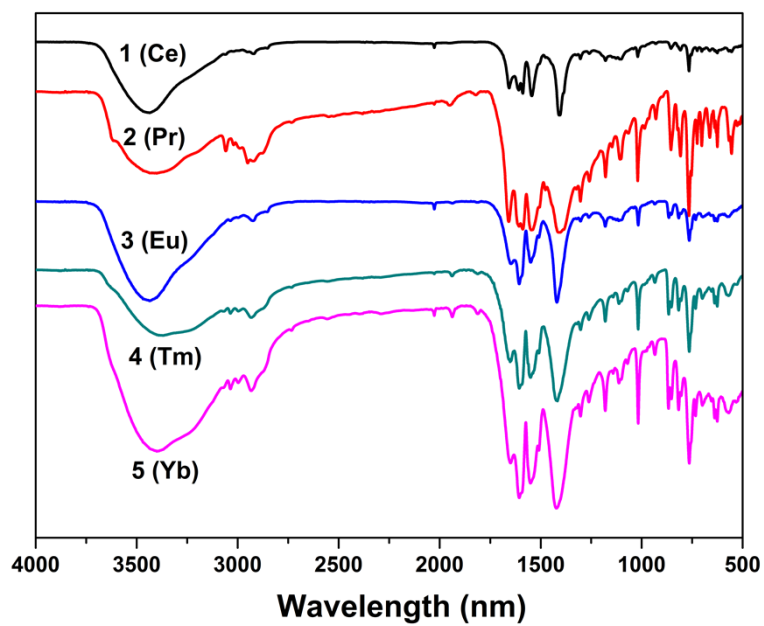


Figure S4. The IR of complexes 1-5.

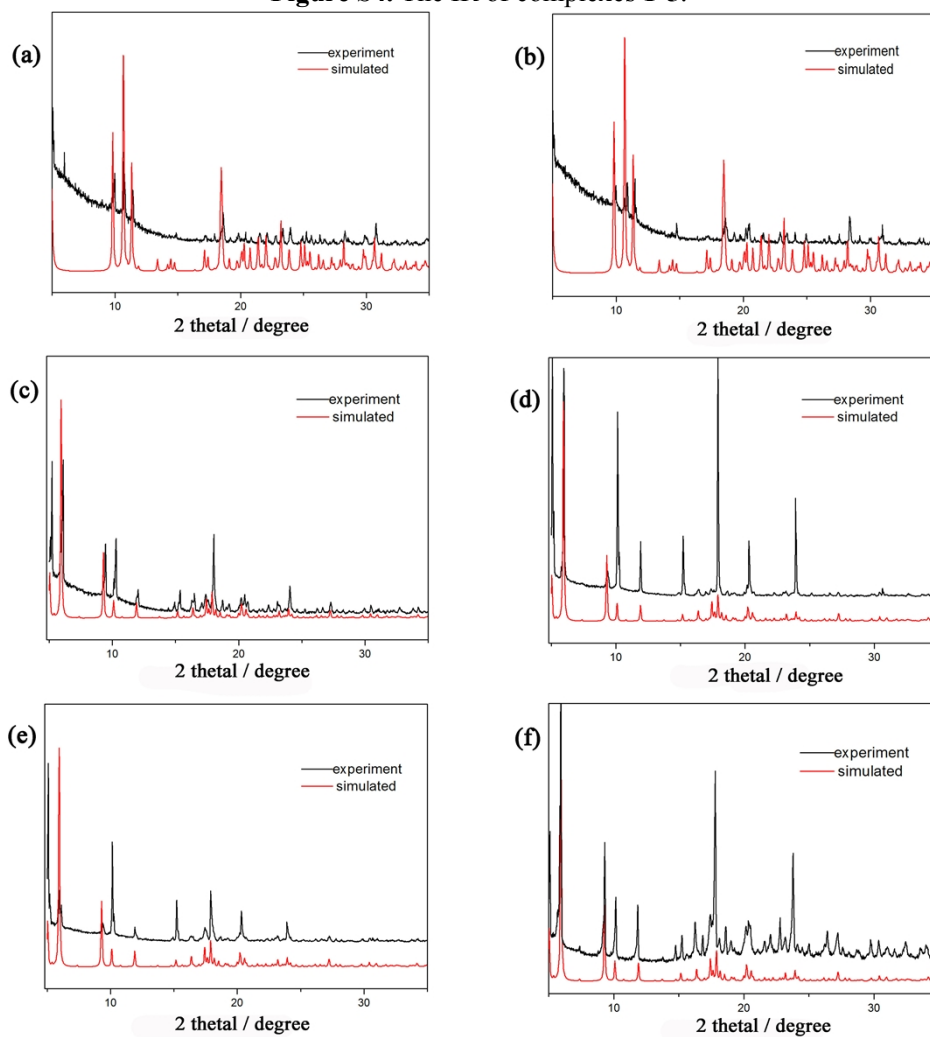


Figure S5. The XRD of complexes 1-5 (a-e) and desolvated 5a (f).

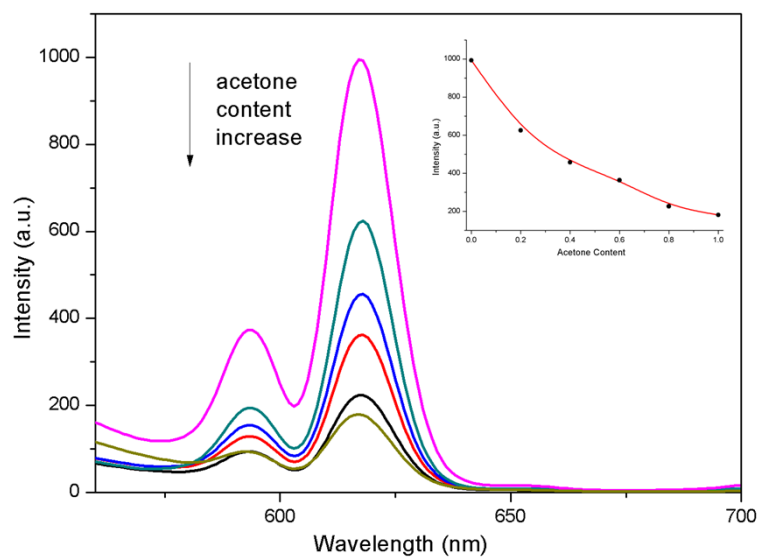


Figure S6. PL spectra of **3 (Eu)** that was introduced into DMSO and acetone mixtures with increasing acetone volume content from 0 to 1 (top-to-bottom). Inset: The PL intensity as a function of acetone volume content.